NISTIR 88-3904

IGNITION CHARACTERISTICS OF THE IRON-BASED ALLOY UNS S66286 IN PRESSURIZED OXYGEN

James W. Bransford
Phillip A. Billiard
James A. Hurley
Kathleen M. McDermott
Isaura Vazquez

Stimulating America's Progress
1913-1988

NISTIR 88-3904

IGNITION CHARACTERISTICS OF THE IRON-BASED ALLOY UNS S66286 IN PRESSURIZED OXYGEN

James W. Bransford
Phillip A. Billiard
James A. Hurley
Kathleen M. McDermott
Isaura Vazquez

Chemical Engineering Science Division
Center for Chemical Engineering
National Engineering Laboratory
National Institute of Standards and Technology
Boulder, Colorado 80303-3328

U.S. DEPARTMENT OF COMMERCE, C. William Verity, Secretary

NATIONAL INSTITUTE OF STANDARDS AND TECHNOLOGY, Ernest Ambler, Director

CONTENTS

List of Figures

List of Tables

Ignition Characteristics of the Iron-Based Alloy UNS S66286 in Pressurized Oxygen

James W. Bransford, Phillip A. Billiard, James A. Hurley,
Kathleen M. McDermott, and Isaura Vazquez

National Institute of Standards and Technology
Boulder, Colorado   80303-3328

The development of ignition and combustion in pressurized oxygen atmospheres was studied for the iron based alloy UNS S66286. Ignition of the alloy was achieved by heating the top surface of a cylindrical specimen with a continuous-wave CO_2 laser. Two heating procedures were used. In the first, laser power was adjusted to maintain an approximately linear increase in surface temperature. In the second, laser power was periodically increased until autoheating (self-heating) was established. It was found that the alloy would autoheat to destruction from temperatures below the solidus temperature. In addition endothermic events occurred as the alloy was heated, many at reproducible temperatures. Many endothermic events occurred prior to abrupt increases in surface temperature and appeared to accelerate the rate of increase in specimen temperature to rates greater than what would be expected from increased temperature alone. It is suggested that the source of these endotherms may increase the oxidation rate of the alloy. Ignition parameters are defined and the temperatures at which these parameters occur are given for the oxygen pressure range of 1.72 to 13.8 MPa (25 to 2000 psia).

Key words: alloys; combustion; ignition; ignition temperature; iron alloy; metals

1

Introduction

A number of serious accidents and catastrophic fires have occurred that involved the ignition and subsequent combustion of metals in oxygen systems. As oxygen system pressure has increased, the potential for disastrous ignition and combustion has also increased. In order to reduce the potential of ignition and combustion failure in oxygen systems, a knowledge of the ignition and combustion characteristics of metals is needed. In recognizing this need, the George C. Marshall Flight Center (MSFC) initiated a program at the National Institute of Standards and Technology (NIST) to study the ignition and combustion characteristics of selected alloys in pressurized oxygen. A list of the alloys that have been studied is given in table 1.

This report, the first in a series, gives the results for the iron-based alloy UNS S66286. The studies involved heating the top surface of specimens of the material by a continuous-wave (cw) CO_2 laser in pressurized oxygen. The surface and interior temperatures were recorded as the specimens were heated. High speed cinematography of the ignition and combustion events was also obtained. From this information the spontaneous ignition (critical) temperature, enhanced oxidation temperature (our terminology), ignition temperature, combustion temperature, ignition/combustion morphology and other information were obtained for the oxygen pressure range of 1.72 to 13.8 MPa (250 to 2000 psia).

Experimental Procedure

Cylindrical test specimens, figure 1, were machined from commercially available age-hardened UNS S66286 alloy. THe ultimate tensile strength of the alloy used was 1100 MPa (160 ksi). The chemical composition of the alloy was 0.17% Al, 0.0065% B, 0.051% C, 14.02% Cr, 0.12% Mn, 1.11% Mo, 24.61% Ni,

Table 1. Materials selected for the determination of ignition and combustion characteristics.

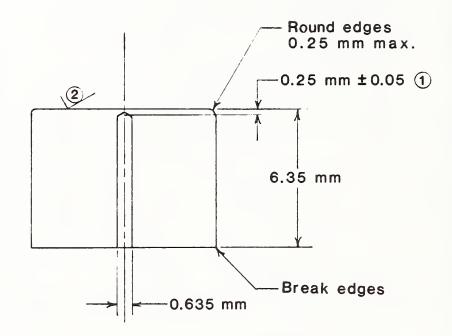| UNS #	Al	C	Co	Cr	Cu	Fe	Mn	Mo	Ni	P	S	Si	Ti	W	Other
A03560	bal.				≤0.25	≤0.60	≤0.35					6.5–7.5	≤0.25		Mg 0.20–0.45; Zn 0.35; Other: ea ≤0.05 total≤0.15
A03580	bal.			0.20	≤0.20	≤0.30	≤0.20		≤0.25			7.6–8.6	0.10–0.20		Be 0.10–0.30; Mg 0.40–0.60; Zn ≤0.20; Other ea ≤0.05 total ≤0.15
N06625	≤0.40	≤0.10		20.0–23.0		≤5.0	≤0.50	8.0–10.0	bal.	≤0.015	≤0.015	0.50	≤0.40		Nb 3.15–4.15
N07001	1.20–1.60	0.03–0.10	12.0–15.0	18.0–21.0	≤0.50	≤2.00	≤1.00	3.50–6.00	bal.	≤0.030	≤0.030	≤0.75	2.75–3.25		B 0.003–0.01; Zr 0.02–0.12
N07718	0.20–0.80	≤0.08	≤1.00	17.0–21.0	≤0.30	bal.	≤0.35	2.80–3.30	50.0–55.0	≤0.015	≤0.015	≤0.35	0.65–1.15		B ≤0.008; Nb 4.75–5.50; Zr 0.02–0.12
N07750	0.40–1.00	≤0.08		14.0–17.0	≤0.50	5.0–9.0	≤1.00		≥70.0		≤0.010	≤0.50	2.25–2.75		Nb 0.70–1.20
N10276		≤0.02	≤2.5	14.5–18.5		4.0–7.0	≤1.00	15.0–17.0	bal.	≤0.030	≤0.030	≤0.05		3.0–4.5	V ≤0.35
S30100		≤0.15		16.0–18.0		bal.	≤2.00		6.00–8.00	≤0.045	≤0.030	≤1.00			
S30200		≤0.15		17.0–19.0		bal.	≤2.00		8.00–10.00	≤0.045	≤0.030	≤1.00			
S30400		≤0.08		18.0–20.0		bal.	≤2.00		8.00–10.50	≤0.045	≤0.030	≤1.00			
S30403		≤0.03		18.0–20.0		bal.	≤2.00		8.00–12.00	≤0.045	≤0.030	≤1.00			
S31600		≤0.08		16.0–18.0		bal.	≤2.00	2.00–3.00	10.00–14.00	≤0.045	≤0.030	≤1.00			
S32100		≤0.08		17.0–19.0		bal.	≤2.00		9.00–12.00	≤0.045	≤0.030	≤1.00	≥5×C		
S34700		≤0.08		17.0–19.0		bal.	≤2.00		9.00–13.00	≤0.045	≤0.030	≤1.00			
S44004		0.95–1.20		16.0–18.0		bal.	≤1.00	≤0.75		≤0.045	≤0.030	≤1.00			
S66286	≤0.35	≤0.08		13.5–18.0		bal.	≤2.00	1.00–1.50	24.0–27.0	≤0.040	≤0.030	≤1.00	1.90–2.35		B 0.001–0.010; V 0.10–0.50
R30188		0.05–0.15	bal.	20.0–24.0		≤3.00	≤1.25		20.0–24.0			0.20–0.50		13.0–18.0	La 0.03–0.15
NARloy A									bal.						Ag 3.5

3

Round edges
0.25 mm max.

—0.25 mm ±0.05 ①

6.35 mm

Break edges

0.635 mm

NOTES:

1. Apex to top surface center.

2. Surface finish as specified.

3. 6.35 mm or 8.00 mm dia.
   as required.

Figure 1. Test specimen configuration.

0.011% P, 0.004% S, 0.15% Si, 2.15% Ti, 0.25% V, with the balance Fe. Specimen dimensions were 6.3 mm (0.25 in) in diameter by 6.3 mm (0.25 in) in height for the linear temperature increase tests and 8.0 mm (0.313 in) in diameter by 6.3 mm (0.25 in) in height for the incremental temperature increase tests. A thermocouple hole was drilled axially to within 0.25 ± 0.05 mm (0.010 ± 0.002 in) of the top surface. The top surface of a specimen was maintained in the "as machined" finish to improve the absorptivity of the surface to the laser beam at the beginning of an experiment and to give a diffuse laser beam reflection which would reduce potential heat damage to the chamber liner.

The experiments were carried out in commercially pure oxygen. Chamber pressure was varied from 1.72 to 13.8 MPa (250 to 2000 psia) in 1.72 MPa (250 psia) steps. The pressure was allowed to increase during the experiments and was recorded at the beginning of specimen combustion. This pressure rarely exceeded the initial chamber pressure by 10 percent.

To assemble an experiment, a specimen was mounted in a machined graphite block and was insulated from the block by packed aluminum oxide powder. This assembly was placed upon a ceramic foam pad which was fixed to a pedestal as shown in figure 2.

The top surface of the specimen was heated by a cw CO_2 laser beam. The laser had been detuned from the pure TEM_{oo} mode so as to contain higher order modes. This procedure distributed the laser power more uniformly within the laser beam and allowed for a more uniform heating of the specimen. The laser beam was focused to cover approximately 80% of the top surface area of the specimen. This allowed the beam to remain predominately on the specimen surface as the beam was randomly refracted by gas convection currents rising from the heated surface.
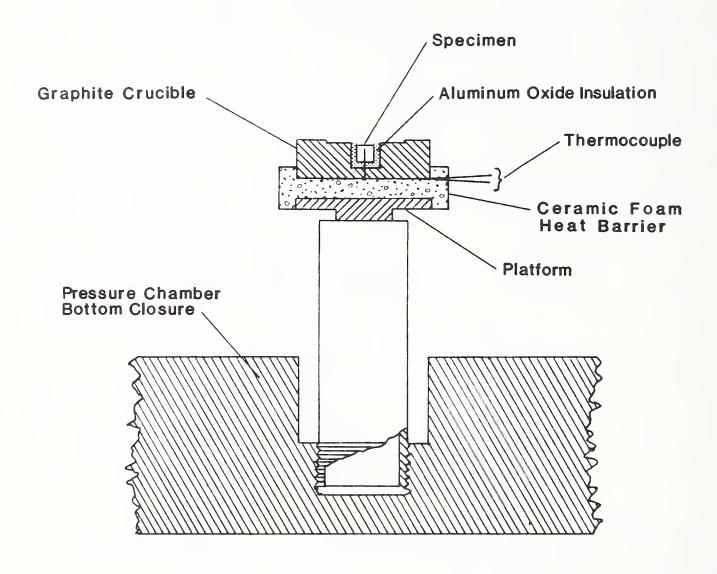
Figure 2. Experimental setup.

Two heating procedures were used in this study. The first procedure established and maintained an approximately linear temperature increase in specimen surface temperature and was called the Linear Temperature Scan (LT) heating procedure. Surface heating rates of 100 K/min were most often used; however, rates of up to 250 K/min were used occasionally. The LTS heating procedure was used primarily to determine if rapidly developing exothermic events were present; but the tendency of a material to autoheat (self-heat), which is a much slower exothermic process, was also detectable.

The second heating procedure incrementally increased the laser beam power. The surface was allowed to reach a short term equilibrium before another increment of power was applied. At some power level during the procedure, the surface temperature would not reach an equilibrium and the material would autoheat to destruction. This procedure was called the Incremental Temperature Scan (ITS) heating procedure.

The principal parameters in this study were the surface temperature and interior temperature of the specimen. The surface temperature was measured using two-color ratio pyrometry. Two pyrometers were ultimately used. One pyrometer covered the temperature range of 973 to 1773 K (1291 to 2732 °F) and had an output range which gave a temperature sensitivity of 8 K/mv (14 °F/mv). The second pyrometer covered the temperature range of 1173 to 2673 K (1652 to 4352 °F) and had an output range which gave a temperature sensitivity of 15 K/mv (27 °F/mv). These signals were recorded by a digital oscilloscope which used 15 bit analog to digital (A/D) converters. These converters have a maximum voltage resolution of 6.25 μv. Thus, the maximum temperature resolution was 0.05 K (0.09 °F) for the 973 to 1173 K range pyrometer and 0.09 K (0.06 °F) for the 1173 to 2673 K range pyrometer. The accuracy of the

7

pyrometers was 1 percent of full scale when viewing black or gray body surfaces.

The pyrometers view the specimen through the pressure chamber windows, figure 3, which are at angle 45 ° from the vertical. The specimen surface observed within the pyrometers' circular measurement field of view was elliptical and comprised top surface dimensions that varied from approximately 5 to 7 mm (0.2 to 0.3 in). The pyrometers did not measure the maximum surface temperature but responded to the overall temperature of the viewed area. The temperature was not an average but was biased toward the highest temperature within the viewed area due to the Stefan-Boltzmann radiation law.

The interior temperature of the specimen was measured using a thermocouple of platinum-versus-platinum 10% rhodium (Type S). The thermocouple was insulated except for the bead, which was in contact with the specimen at the top of the thermocouple well. The output of the thermocouple was referenced to a 273 K cold junction and then digitized directly at the maximum sensitivity of the digitizer, 6.25 μv. This gave a temperature sensitivity of approximately 0.6 K (1 °F) over the temperature range of interest, 773 to 1773 K. The thermocouple junction temperature uncertainty did not exceed 0.5 K from 273 to 1373 K. From 1373 to 1723 K, the uncertainty increased but did not exceed 2 K at 1723 K.

Special tests, in which the thermocouple was spot welded to the top surface, were also run. These tests were used to obtain estimates of the temperature of the alloy/oxide interface.

The Metal Ignition Process

A detailed description of the ignition process of metals involves a significant number of parameters. However, a general understanding of the

8

Laser Beam

Polycrystalline
NaCl Window

Observation
Windows (4)

Sapphire
Window

Quartz
Splatter
Shield

Access
Ports
or
Windows
(4)

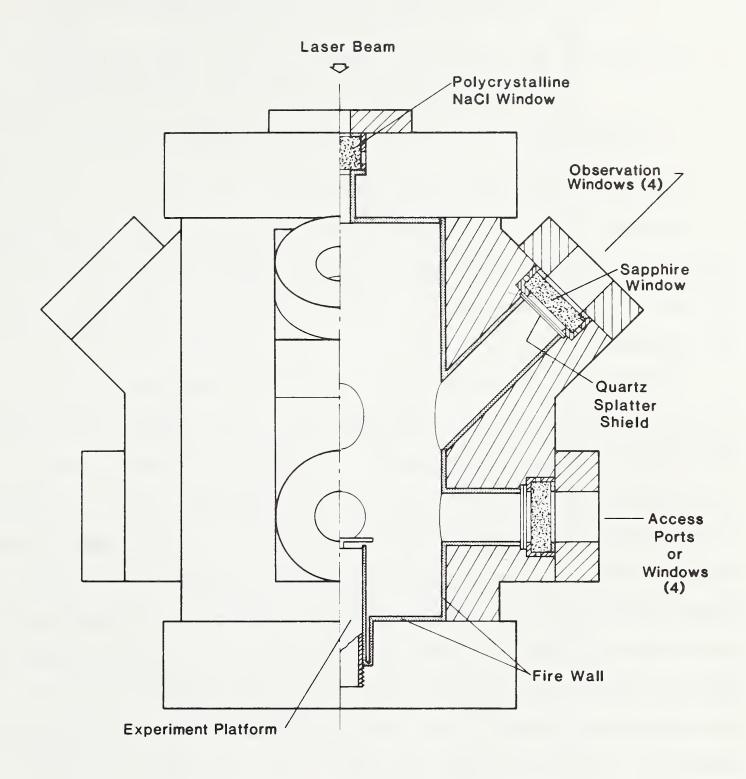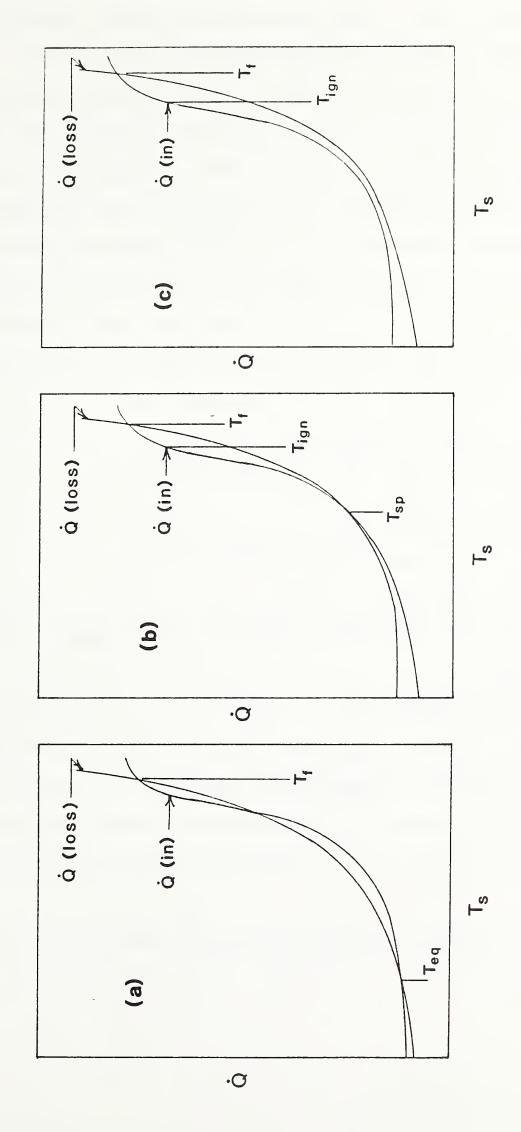Fire Wall

Experiment Platform

Figure 3. Test chamber configuration.

process can be obtained by considering a simple generalized heat balance for an oxidizing surface. The parameters that need to be incorporated are:

1. $\dot{Q}$(loss) - the rate of heat loss from the oxidizing surface by conduction, convection and radiation;

2. $\dot{Q}$(ext) - the rate of heat transferred to the oxidizing surface from external sources by conduction, convection and radiation;

3. $\dot{Q}$(chem) - the rate of heat generation by oxidation of the alloy;

4. $\dot{Q}$(in) - the sum of $\dot{Q}$(ext) and $\dot{Q}$(chem).

To further simplify the process, $\dot{Q}$(ext) will be a constant, but different, value for each of the illustrations in figure 4. Both $\dot{Q}$(loss) and $\dot{Q}$(chem) are functions of surface temperature and other parameters which are constant for this discussion.

An initial application of $\dot{Q}$(ext), which is less than that required to initiate ignition, will increase the magnitude of $\dot{Q}$(in) to some value greater than $\dot{Q}$(loss). The surface temperature, T_s, will then increase to some equilibrium value, T_{eq}, as shown in figure 4a. Since the slope of the $\dot{Q}$(in) curve is less than the slope of the $\dot{Q}$(loss) curve at T_{eq}, the oxidizing surface temperature cannot increase on its own beyond T_{eq} because the increase in heating rate will be less than the increase in cooling rate at temperatures greater than T_{eq}. Thus, a stable surface temperature is reached. However, the degree of stability over time will depend upon whether the surface is undergoing time dependent or time independent oxidation. If time dependent oxidation is occurring, $\dot{Q}$(chem) will decrease with time and the oxidizing surface temperature will also decrease with time. If time independent oxidation is occurring, $\dot{Q}$(chem) will remain constant and the oxidizing surface temperature will remain constant if all other parameters remain constant.

10

Figure 4. General variation of heat balance parameters as a function of surface temperature.

11

As $\dot{Q}$(ext) is systematically increased, an equilibrium surface temperature will ultimately be reached at which the slope of the $\dot{Q}$(in) curve equals the slope of the $\dot{Q}$(loss) curve, figure 4b. This equilibrium temperature is defined as the spontaneous ignition (or critical) temperature, T_{sp}. Since $\dot{Q}$(chem) and $\dot{Q}$(loss) both increase with increasing temperature, the slopes of the $\dot{Q}$(in) and $\dot{Q}$(loss) curves may be approximately equal over a fairly wide temperature range. This range we have previously described as a quasi-stable temperature region [1]. The behavior of an alloy within this region is of considerable interest. Small shifts in other parameters which cause perturbations in any of the heat gain or heat loss parameters, can cause the oxidizing surface to either cool or autoheat. When $\dot{Q}$(in) is sufficiently large for spontaneous ignition to occur, several parameters may be defined. They are:

1. Spontaneous ignition temperature, T_{sp}--the temperature at which $d\dot{Q}(in)/dT_s = d\dot{Q}(loss)/dT_s$;

2. Ignition temperature, T_{ign}--the temperature at which $[\dot{Q}(in)-\dot{Q}(loss)]$ = maximum;

3. Flame temperature, T_f--the maximum temperature reached by the oxidizing surface.

These parameters are shown in figure 4b.

Equilibrium surface temperatures, greater than T_{sp}, may be established by decreasing $\dot{Q}$(ext) once the surface temperature has exceeded T_{sp}. However, these equilibrium surface temperatures must be considered unstable since the tendency is for the alloy to autoheat; i.e., the slope of the $\dot{Q}$(in) curve is greater than the slope of the $\dot{Q}$(loss) curve.

At this point it is useful to consider the effect of physical state on the parameters that have been introduced. In general, the oxidation rate of the

12

solid alloy is less than that of the liquid alloy. Therefore, if T_{sp} occurs

while the alloy is solid, phase dependent parameters may be defined. However,

defining ignition parameters for the liquid phase in our experiments was

difficult because of fluid flow effects. When an oxidizing fluid moves, the

rate of oxygen transport to the oxidizing surface may be significantly

increased for a short time interval. This in turn increases the rate of

material consumption, which increases the surface temperature for the flow

interval. The net result of the fluid movement is to break up the overall

smoothness of the $\dot{Q}$(chem) curve, which make it difficult to separate movement

enhanced oxidation effects from quiescent oxidation effects. For this reason,

liquid phase ignition parameters were not determined for the ITS heating

procedure (with the exception of the temperature at the beginning of

combustion, T_{cmb}); only solid phase ignition parameters were determined.

If $\dot{Q}$(ext) is sufficiently large, the $\dot{Q}$(in) curve will not intersect the

$\dot{Q}$(loss) curve until T_f is reached, figure 4c. In this case T_{sp} is not

obtainable from the experiment; however, T_{ign} and T_f are. It is interesting

to note that T_{ign} does not differ in this case from the case shown in figure

4b. This is due to the definition of T_{ign} as being the temperature at the

maximum deviation between the $\dot{Q}$(in) curve and the $\dot{Q}$(loss) curve. This means

that our experiments, using the ITS heating procedure, can be thermally

overdriven without seriously affecting the value of T_{ign}. This statement

assumes that the excess external heat input is moderately more than the minimum

required to achieve ignition and not orders of magnitude more.

Since the exact shape and magnitude of the $\dot{Q}$(in) and $\dot{Q}$(loss) curves are

now known, the determination of the ignition parameters must be based upon

other measurable parameters. In our case the surface and interior temperatures were used.

To determine the spontaneous ignition temperature an apparent changing emissivity contribution to specimen heating had to be separated from the oxidation contribution. This was accomplished by running a number of tests using preoxidized specimens. These tests, when compared to the standard test, showed that the apparent emissivity contribution to the specimen heating rate, under constant laser power, was linear or nearly linear, as shown in the Appendix. Since the oxidation rate of metals and alloys is nonlinear with temperature, spontaneous ignition was assumed to have occurred when the temperature-time waveform became nonlinear under constant laser power input, figure 5. The temperature at the beginning of the nonlinear data was taken as the spontaneous ignition temperature.

We have defined an additional ignition parameter that is specific to our data. This parameter defines the beginning of a region on the ITS temperature-time waveform where an abrupt change in curvature occurs prior to ignition, figure 5. The region generally contains a number of abrupt changes in temperature which appear in conjunction with endothermic events. Since it appears that many endothermic events are associated with the abrupt temperature changes, it was postulated that the source of these events increased or enhanced the oxidation rate of the alloy. Thus, the temperature at the beginning of this region has been called the enhanced oxidation temperature, T_{eo}. T_{eo} also appears to be associated with the beginning of the rapid buildup of the oxide layer.

The ignition temperature was the most straightforward parameter to determine since the definition of this parameter implies the existence of a
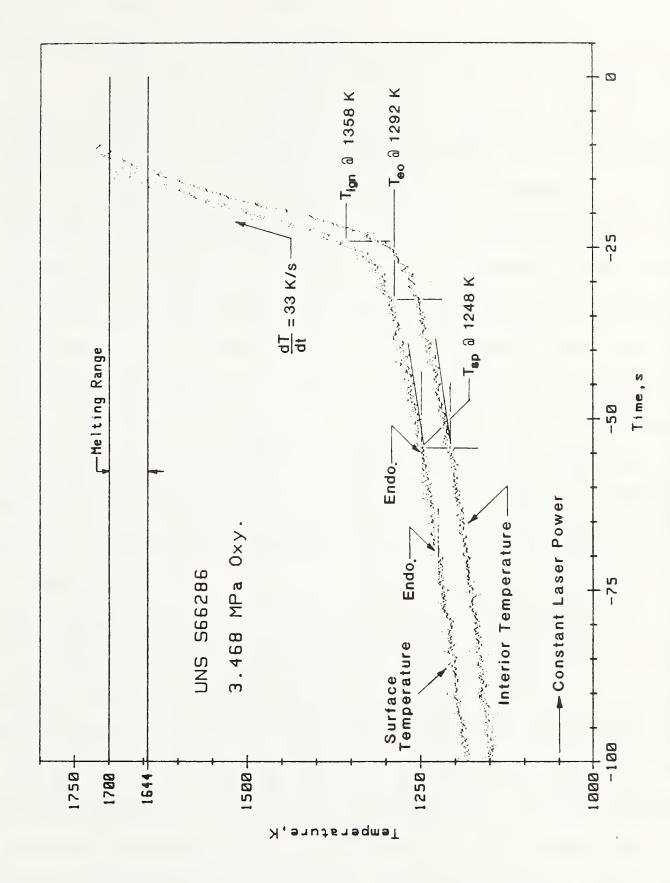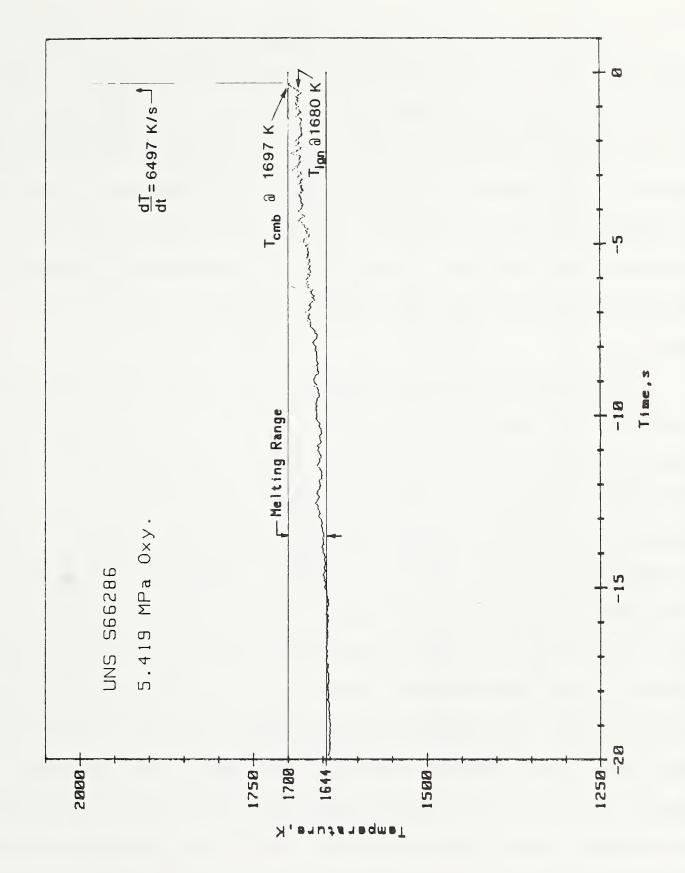
Figure 5. Development of ignition during an ITS test.

15

maximum heating rate of the specimen. This was assumed to have occurred when the maximum rate of change in surface temperature occurred; i.e., $[\dot{Q}(in) - \dot{Q}(loss)] = $ maximum when $dT_s/dt = $ maximum. T_{ign} was the beginning of the region of maximum rate of change in surface temperature, figure 5.

A number of factors can influence the shape and magnitude of the $\dot{Q}(in)$ and $\dot{Q}(loss)$ curves. The $\dot{Q}(loss)$ curve alone can be easily modified by improving or impeding heat transfer from the oxidizing interface. The $\dot{Q}(in)$ curve may be modified by the existence of fluid oxide phases (which may exist above certain temperatures) at the oxidizing interface. These phases may increase the oxidation rate of many alloys [2,3]. The $\dot{Q}(in)$ curve is also modified when the oxidation changes from protective (time dependent) to nonprotective (time independent). When either the $\dot{Q}(in)$ or $\dot{Q}(loss)$ curve is changed, the values of the ignition parameters will also change. In general, the lower the heat transfer rate from the oxidizing surface, the lower the temperature at which T_{sp}, T_{eo}, and T_{ign} will occur; conversely, the greater the heat transfer rate, the higher the temperature at which T_{sp}, T_{eo} and T_{ign} will occur.

Under certain experimental conditions or at elevated oxygen pressures, combustion may develop abruptly before the above defined T_{ign} occurs as shown in figure 6. These abrupt combustions may be due to cracking or spalling of the surface oxides which expose unoxidized or partially oxidized material. (The surface oxides may also be impeding the transfer of oxygen to the oxidizing surface). The resulting rapid increase in oxidation rate that may occur may produce sufficient heat, in a region of restricted heat loss, to melt a small volume of the alloy. This may result in immediate combustion or in a small combustion region which rapidly expands. This type of event has

Figure 6. Abrupt ignition and combustion event during an LTS test.

17

also been called ignition, thus creating an unavoidable dual definition for T_{ign}.

The terms combustion and combustion region are used in this report. This terminology classically means vapor phase combustion (oxidation). For the SS66286 alloy, vapor phase combustion does not occur. For this alloy, and most other alloys listed in table 1, combustion is the fluid flow enhanced oxidation of the liquid alloys. This type of fluid oxidation generates very high temperatures, 2500 K and higher, and develops in milliseconds. The beginning of the development of these very high temperatures is called the combustion temperature, T_{cmb}, and is shown in figure 6.

Results

1. <u>Linear Temperature Scan Tests</u>: The initial experiments in the evaluation of the ignition characteristics of the S66286 alloy were carried out using the LTS heating procedure. Heating rates of approximately 100 K/min were used in order to determine if the alloy had any tendency to develop solid phase ignition to combustion events that would occur in the millisecond to second time period as occurs in some metals and alloys. Experimental data were obtained for the oxygen pressure range of 1.7 MPa (250 psia) to 6.9 MPa (1000 psia). The results for a typical experiment are shown in figure 7. Two waveform features are immediately obvious. The first is the rapid increase in the rate of change in temperature at approximately -30 s and the second is the abrupt ignition with immediate combustion above the liquidus temperature. (Negative time in our data indicates time prior to the start of combustion). Not as obvious, due to the compression of the data, are endothermic (constant temperature) features in the waveform, examples of which are shown in figure 8.
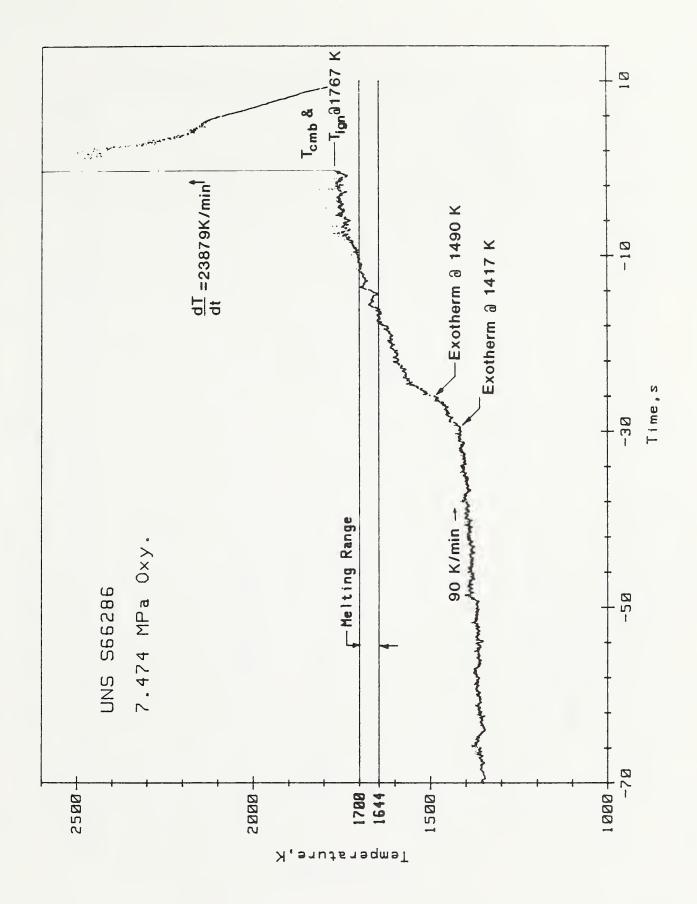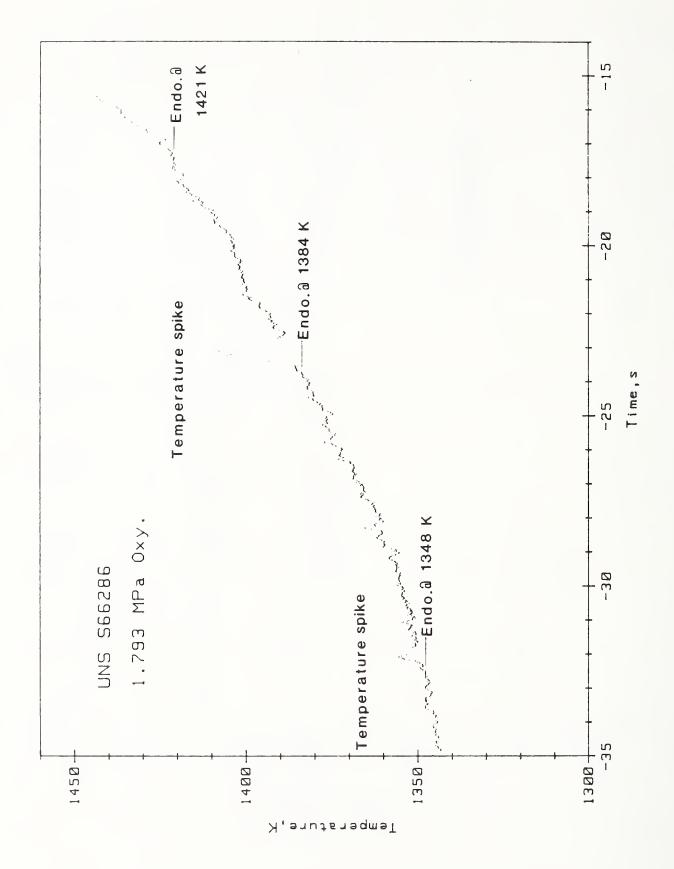
18

Figure 7. Typical surface temperature waveform from an LTS test.

Figure 8. Surface temperature waveform features from an LTS test.

UNS S66286

1.793 MPa Oxy.

Temperature spike

Temperature spike

Endo.ə 1421 K

Endo.ə 1384 K

Endo.ə 1348 K

Temperature,K

Time, s

These features generally had a short duration due to the temperature scan rate used in the experiments.

The rapid increase in the rate of change in temperature, figure 7, starting at approximately -30 s was considered to be due to a rapid increase in oxidation rate of the alloy; this caused the specimen to autoheat faster than control of the heating ramp could offset. However, as laser power was reduced, the heating ramp was eventually re-established (although at a different rate). In most tests, the autoheating appeared to develop in conjunction with endothermic events.

Endothermic events also appeared at other temperatures and often appeared to increase the rate of change in specimen temperature. Also, they were often associated with the development of temperature spikes, rapid exothermic events, ignition and the beginning of combustion.

The temperature spikes, such as shown in figure 8, were attributed to the presence of foreign particles or by particles produced by the fracturing or spalling of the oxide layer which would occur from mechanical stress such as occurs from the normal oxidation of the alloy. A loose particle would have poor thermal contact with the specimen surface and therefore would be heated to high temperatures by the laser beam. A temperature spike would be generated when the temperature of the particle began to affect the pyrometer signal. The spike would disappear when the particle either vaporized or was melted, adhered to the oxide layer, and cooled to the baseline surface temperature. The shapes of the two spikes shown in figure 8 indicate that the particle heated, melted, re-adhered to the substrate and then cooled to the baseline temperature. However, the source of the endotherm that produced the first spike appears to have increased or contributed to the increase in the oxidation rate of the

alloy. Temperature spikes did not appear to affect the oxidation rate of the alloy since permanent changes in the baseline temperature did not occur.

Rapid exothermic events, however, caused permanent changes in the baseline temperature, figure 7. These events were usually abrupt, occurring within miliseconds to several hundred milliseconds. They were often preceded by an endotherm. Exothermic events are considered to be caused by rapid changes in oxidation rate of the alloy.

At an oxygen pressure of 1.7 MPa (250 psia) the development of combustion from ignition occurred over a period of seconds, usually between 5 and 10 s. However, at an oxygen pressure of 3.4 MPa (500 psia) or greater, the development of combustion from ignition occurred within milliseconds, the second major feature of figure 7. In all cases ignition occurred when the surface temperature was within or above the alloy melting range. The ignition data for the LTS test are plotted in figure 9 and are listed in table 2. Figure 10 shows the temperature at which the specimen began to collapse and fluid-flow-enhanced oxidation (combustion) began. These data are also listed in table 2.

It was clear that exothermic events occurred while the alloy was in the solid state; but they did not develop into ignition, at least to oxygen pressures up to 6.9 MPa (1000 psia). These events appear to involve the release of heat, since an increase in the baseline temperature or ramp rate follows their occurrence. We concluded that the exotherms are due to a rapid change in oxidation rate of the alloy. Since endotherms are often involved, it seemed reasonable to assume that the oxidation rate of the alloy was affected by the source of these events. However, the mechanism has not yet been established. As the alloy specimen begin to melt, abrupt ignition to
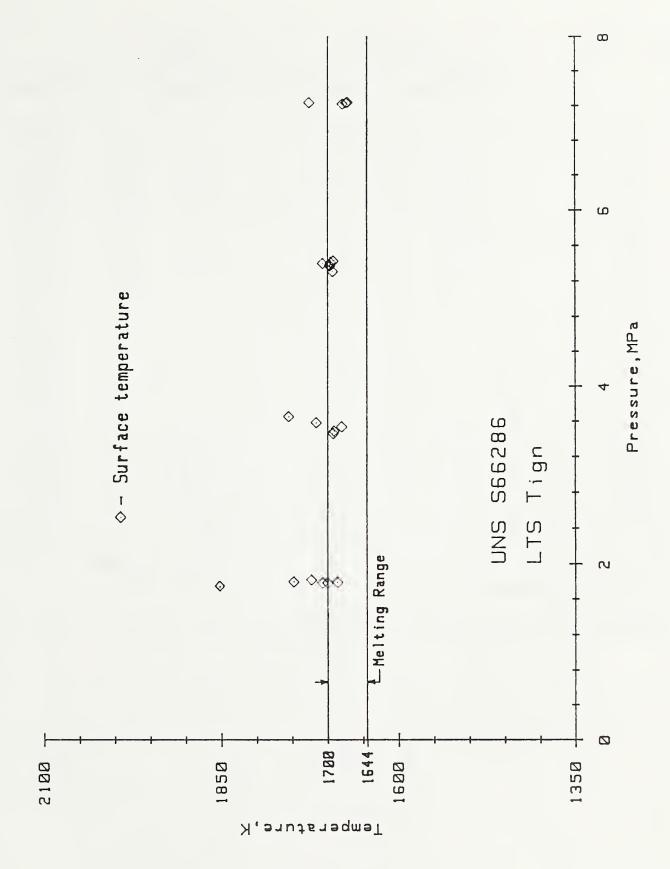
Figure 9. Ignition temperature vs. oxygen pressure from the LTS tests.

Table 2. LTS ignition and combustion temperatures.

Pressure, MPa	T_{ign}, K		T_{cmb}, K	
	Interior	Surface	Interior	Surface
1.793		1877		2009
1.793		1699		1992
1.793	1647	1706	1786	1864
1.800	1658	1685	1788	1985
1.806	1678	1747	1855	1893
1.827	1643	1722		1929
3.468	1674	1691	1771	1759
3.496	1610	1690	1629	1719
3.544		1679		1780
3.592		1715		1756
3.661		1754		1754
5.316		1692		1692
5.378		1696		1696
5.392		1696		1696
5.405		1706		1706
5.419		1695		1695
5.433	1688	1691	1688	1691
7.226	1646	1678	1646	1678
7.239	1631	1725	1631	1725
7.246	1663	1671	1663	1671
7.474	1672	1760	1672	1760

T_{ign} - Ignition temperature

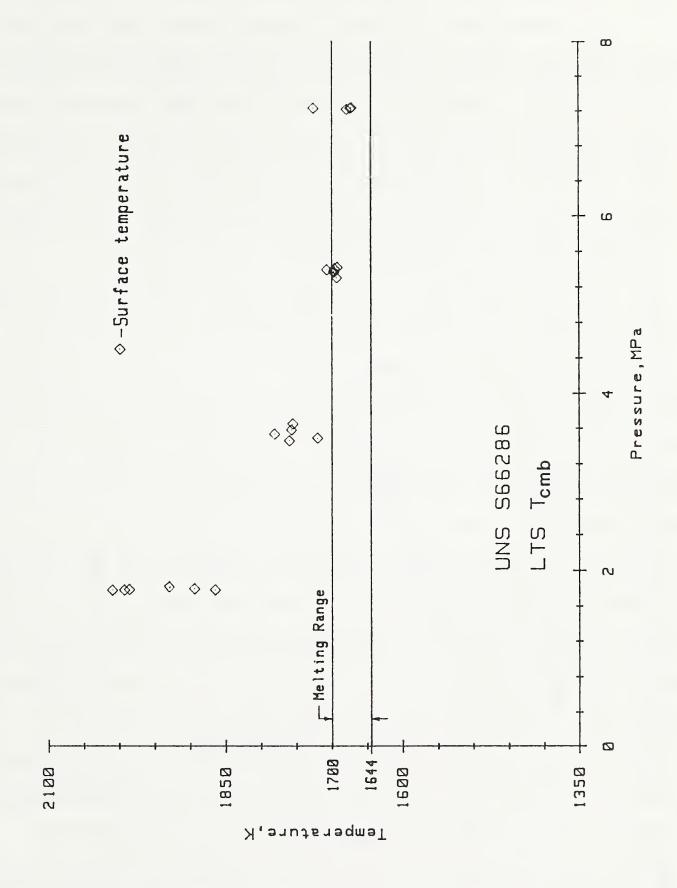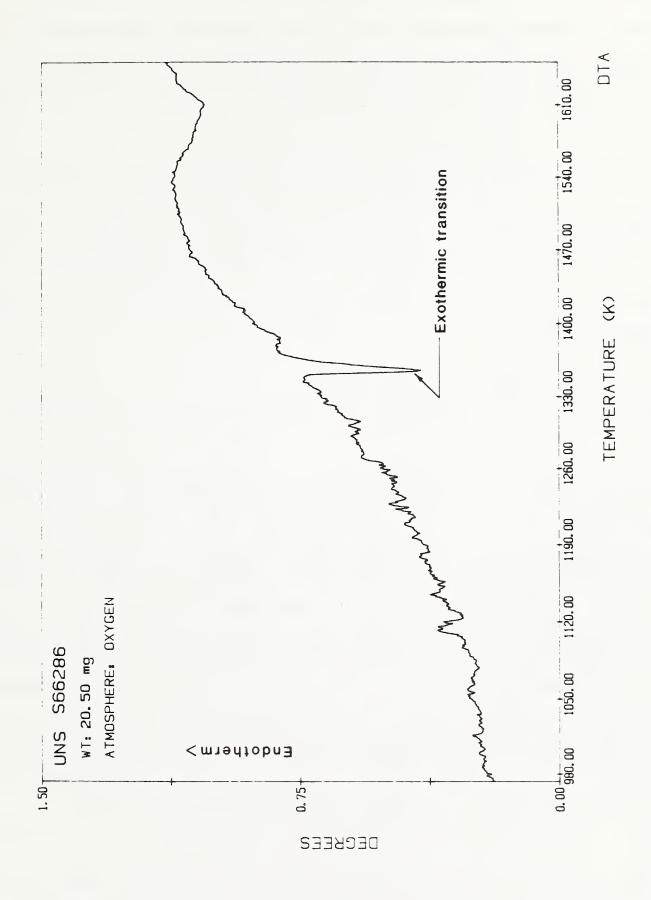T_{cmb} - Temperature at the beginning of combustion

Figure 10. Combustion temperature vs. oxygen pressure from the LTS tests.

25

combustion transitions occurred. These transitions were thought to occur as the upper surface cracked or ruptured from the expansion of the liquefying alloy. It also appeared that the rate of oxidation of the alloy increased significantly as the surface temperature entered the 1300 to 1450 K temperature range. The rate of the temperature increase in this range suggested that the alloy could autoheat to destruction. Because of this tendency, a series of experiments was run to investigate this phenomena. Also, standard differential thermal analysis (DTA) studies were made on oxidizing samples of the alloy.

    2. Differential Thermal Analysis Studies:

The appearance of features in the temperature-time waveform from the LTS tests, interpreted as endothermic and exothermic events, led to efforts to verify this interpretation. The approach was to use standard Differential Thermal Analysis (DTA) techniques and equipment to search for endothermic and exothermic events. Testing was carried out using 15 to 50 mg specimens heated to temperatures above the lower melting range of the alloy in flowing oxygen or helium at atmospheric pressure.

The tests in helium provided a baseline for comparison to the oxidation tests. These tests produced featureless thermographs except for the melting transition. However, the tests in oxygen demonstrated that the oxides produced during heating exhibited considerable thermal activity as shown in figure 11. In fact, so much thermal activity was present that the data were not interpretable. It was clear that endothermic transitions were present but the temperatures of the individual transitions could not be firmly established. The presence of liquid and probably gaseous oxides was evident from the discoloration, and eventual destruction, of the aluminum oxide sample holders.

Figure 11. DTA thermograph produced by heating a specimen of UNS S66286 alloy in oxygen.

27

Several investigators have postulated or observed the presence of liquid oxides during the high temperature oxidation of alloys [2,3]. These investigators have also observed increased oxidation rates when liquid oxides were present. This tended to corroborate our observations of apparently increased oxidation rates at temperatures where many endothermic transitions occurred.

These studies also corroborate the existence of low energy release exotherms and the existence of at least one high energy exothermic event as shown in figure 11. It also provides an independent verification that the alloy does tend to autoheat to destruction at temperatures below the solidus temperature of the alloy.

3. Incremental Temperature Scan Tests:

The experiments to investigate the tendency of the alloy to autoheat to destruction used the ITS heating procedure. This procedure applied a constant heating rate, increased at intervals after surface temperature equilibrium was established, until the alloy specimen began to autoheat. The external heating rate was then held constant until autoheating ceased or combustion occurred. Figure 12 shows the surface and interior temperature-time waveforms after the last power increment, at -165 s, for a typical experiment. (In our figures, the interior temperature waveform data is always terminated at the thermocouple failure point. This point usually occurs at temperatures slightly above the liquidus temperature.) These waveforms clearly show the endothermic regions that had been suggested or very small in the waveforms from the LTS experiments. The effect of the endothermic regions upon the rate of increase in specimen temperature is also evident in the ITS waveforms. These features and their effects are more clearly shown in figures 13 and 14, which are
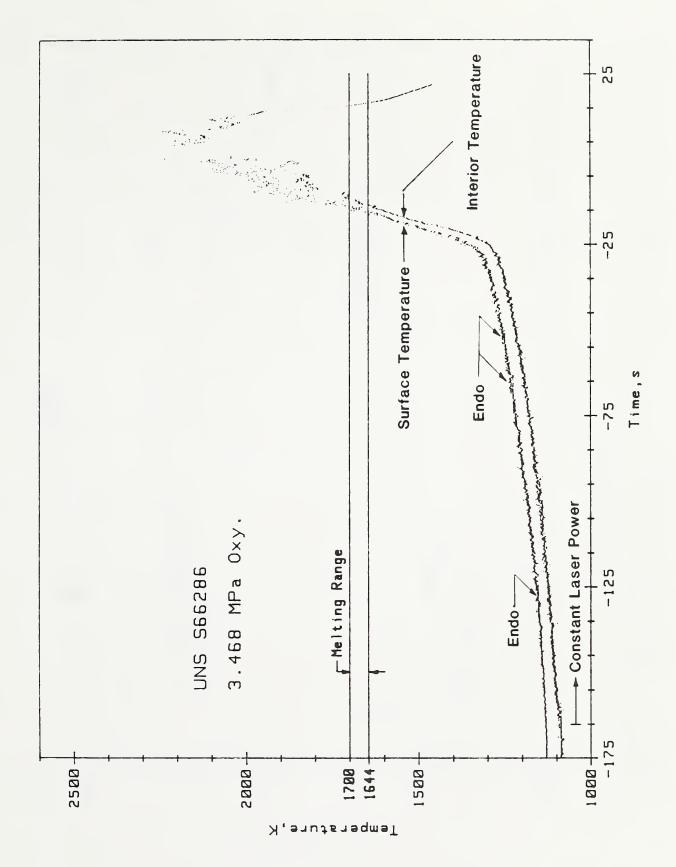
Figure 12. Typical surface and interior temperature waveforms from an ITS test.
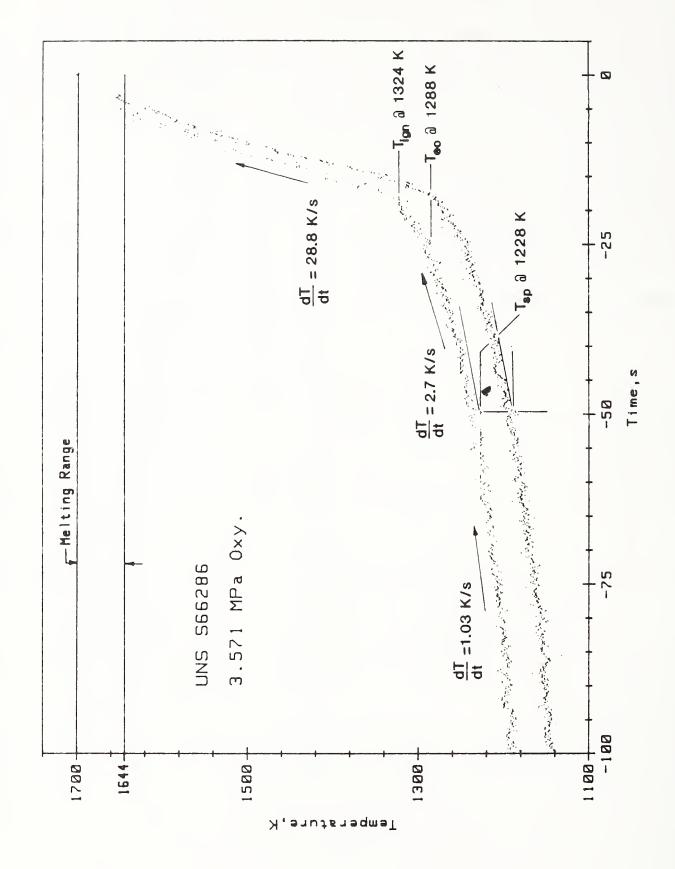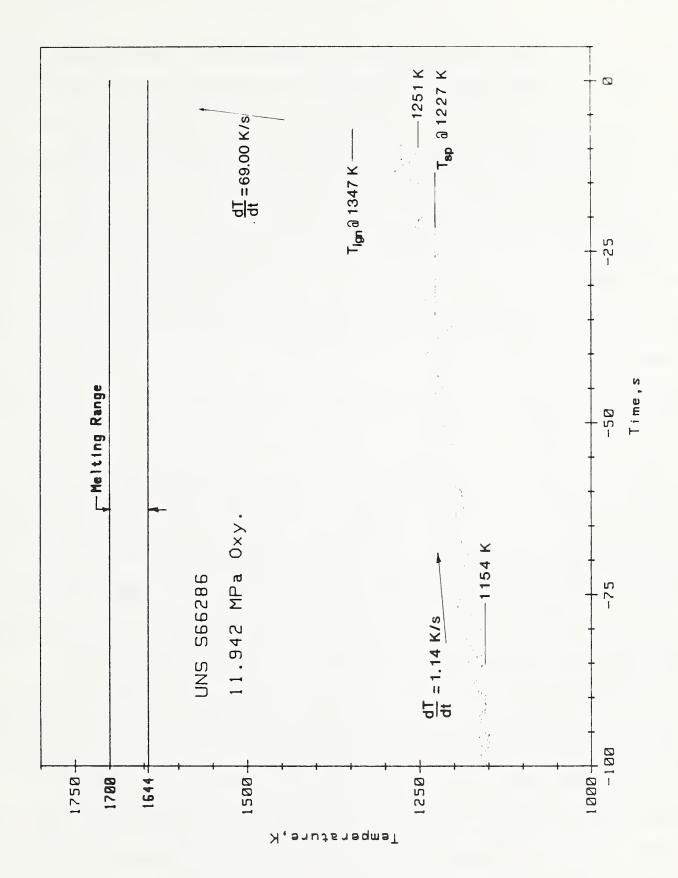
29

Figure 13. Development of ignition in 3.57 MPa oxygen from an ITS test.

30

Figure 14. Development of ignition in 11.94 MPa oxygen from an ITS test.

31

expansions of waveform sections, chosen for their clarity, from several experiments.

Figure 13 shows the rate of increase in temperature, approximately 1 K/s, after the last power increment. This initial autoheating was due primarily to the increasing absorptivity of the surface to the laser radiation; see Appendix. An oxidation component to the heating rate was also present but very small. However, as the specimen temperature increases, the oxidation component to the heating rate steadily increases at a nonlinear rate. The oxidation component ultimately becomes the principal heat source governing the rate of increase in specimen temperature at the spontaneous ignition temperature. The very slight curvature in the temperature-time waveforms between -100 s and T_{sp} was considered to be due to the increasing oxidation component to the heating rate. T_{sp} was chosen as the beginning of the temperature-time waveform section where it appeared clear that oxidation heat input to the system was the dominate factor in increasing the specimen temperature. This was the beginning of the clearly nonlinear section of the temperature-time waveform.

Figure 14 shows the effect of increased oxygen pressure on the rate of increase in temperature. As can be seen the rate of temperature increase prior to T_{sp} was approximately the same as in the much lower oxygen pressure experiment shown in figure 13. This was additional evidence that the heating rate at temperatures below T_{sp} was due primarily to increasing absorptivity of the developing oxide layer to the laser radiation. The effect of the endothermic regions was also clearer at the higher oxygen pressures. Also, the rate of increase in temperature after T_{ign} was greater than twice the values of those shown in figures 12 and 13.

32

After spontaneous ignition was achieved, the specimen temperature began to slowly increase. This increase was usually followed by a series of rapid step increases in temperature which were associated with endothermic features. The net result of these step increases was an abrupt change in curvature of the temperature-time waveform. An attempt was made to quantify the onset of this abrupt change in curvature by relating it to the temperature of features in the temperature-time waveform. Since it is our premise that the endothermic features are associated with rapid changes in the oxidation rate of the alloy, this temperature was called the enhanced oxidation temperature, T_{eo}. After T_{eo} has occurred the rate of change in temperature continued to increase until a maximum was reached. The temperature at which this maximum rate of change in temperature occurred was considered to be the temperature at which the maximum deviation between the $\dot{Q}(in)$ and $\dot{Q}(loss)$ curves occurred. Thus, this temperature was taken as the ignition temperature, T_{ign}. The values of the ignition parameters--T_{sp}, T_{eo} and T_{ign}--are listed in table 3 and plotted as a function of oxygen pressure in figures 15, 16, and 17. The data was fitted to linear least-squares curves so that the trend of the data could be established. The slope of the trend lines are noted on the plots.

An attempt was made to estimate the temperature of the oxidation zone by spot welding a thermocouple of Pt vs. Pt 10% Rh to the top center of several specimen. Typically, it was found that the thermocouple measurement was approximately 40 K below the pyrometer at spontaneous ignition. This difference decreased to approximately 30 K at ignition. After ignition, the difference approached approximately 10 K as the alloy began to melt. These estimates were made at oxygen pressures of 1.7 and 3.4 MPa (250 and 500 psia) and are probably not valid for higher oxygen pressures.
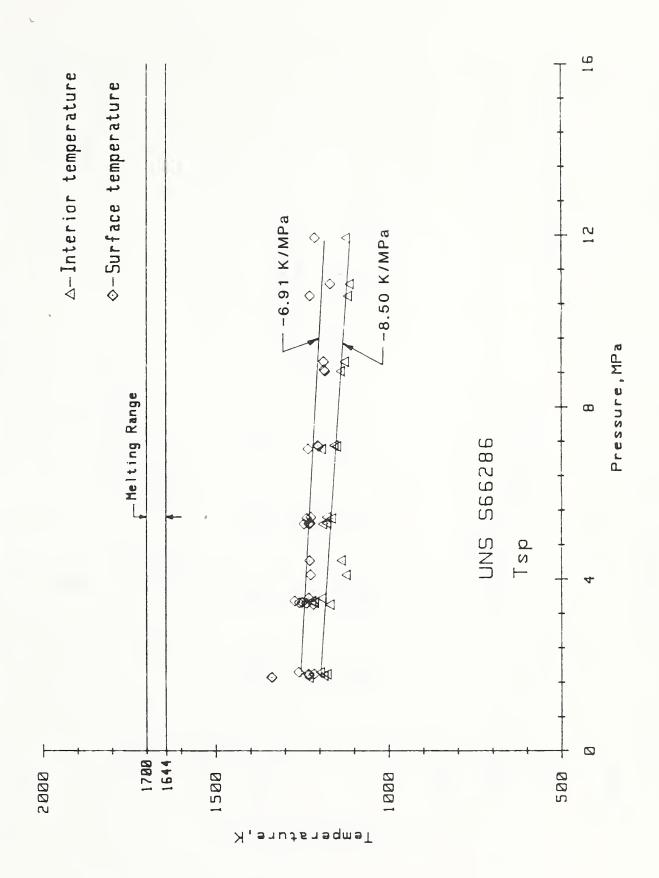
Table 3. ITS ignition parameter temperatures

Pressure, K	Tsp, K		Te$_o$, K		T$_{ign}$, K	
	Interior	Surface	Interior	Surface	Interior	Surface
1.724	1224	1335	1267	1383	1299	1421
1.772	1181	1228	1267	1324	1308	1384
1.806		1229		1271		1319
1.806	1172	1213	1225	1261	1334	1370
1.848	1191	1258	1205	1274	1237	1321
3.420	1163	1215	1200	1252	1293	1367
3.447		1235		1253		1389
3.461		1256		1292		1433
3.468	1208	1248	1252	1292	1312	1358
3.503	1216	1269		1327		1369
3.571	1186	1228	1239	1288	1280	1324
4.109	1116	1223	1132	1238	1252	1397
4.440	1130	1226	1153	1249	1185	1293
5.288	1184	1242	1225	1282	1239	1302
5.295		1228		1260		1348
5.309	1172	1224	1218	1259	1284	1344
5.419	1158	1234	1208	1291	1266	1373
5.447	1173	1222	1199	1257	1257	1318
7.033	1187	1230	1208	1246	1279	1321
7.095	1143	1200	1184	1242	1255	1348
7.115	1151	1202	1253	1290	1314	1364
8.839	1132	1181	1145	1193	1189	1284
8.867		1184		1250		1334
9.060	1120	1185	1149	1228	1176	1289
10.590	1111	1225	1135	1254	1179	1326
10.866	1106	1166	1130	1180	1306	1408
11.942	1117	1211	1144	1227	1227	1344

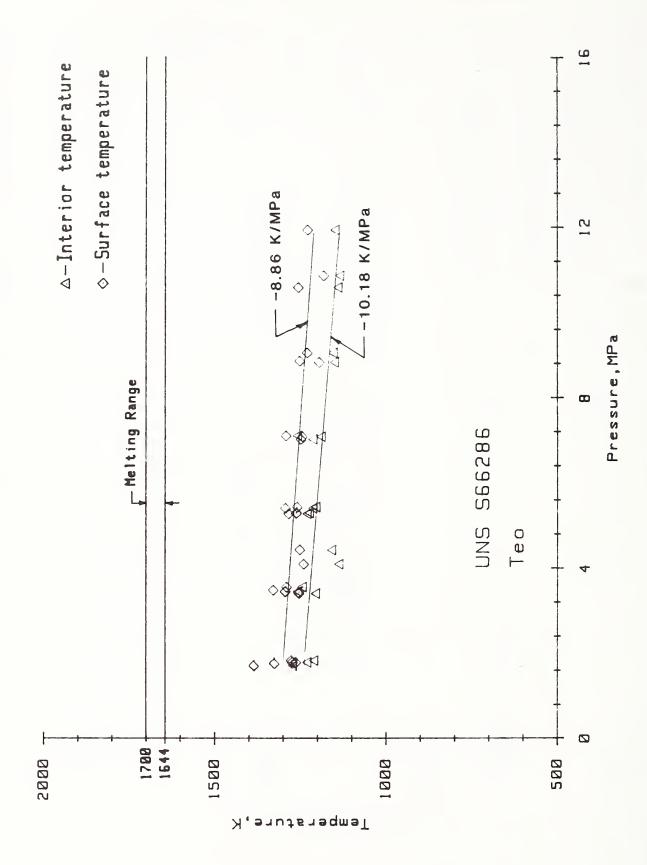T$_{sp}$ - Spontaneous ignition temperature.

T$_{eo}$ - Enhanced oxidation temperature.

T$_{ign}$ - Ignition temperature.

Figure 15. Spontaneous ignition temperature vs. oxygen pressure from the ITS tests.

Figure 16. Enhanced oxidation temperature vs. oxygen pressure from the ITS tes
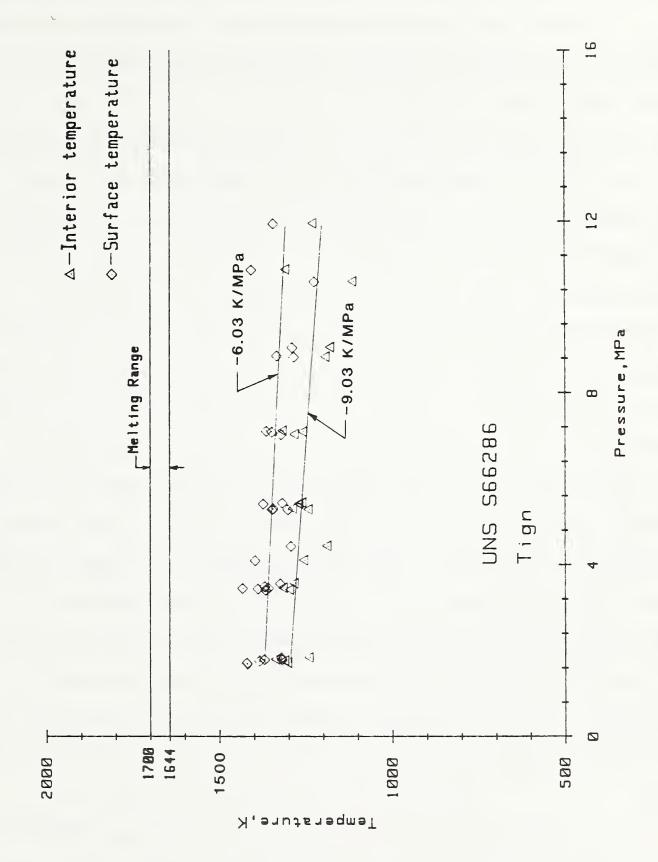
36

Figure 17. Ignition temperature vs. oxygen pressure from the ITS tests.

4. Data Accuracy:

The surface temperature values of T_{sp}, T_{eo}, and T_{ign} were determined with a commercial two-color ratio pyrometer with an accuracy of 1 percent when measuring black-or gray-body temperatures. This was verified by calibration using a NBS standard lamp.

The assumption made in two-color ratio pyrometry is that the change in emissivity over the measurement wavelength band is negligibly small. However, oxidizing surfaces are notorious for the variation in the value of emissivity with wavelength. To determine whether or not a pyrometer measurement problem existed, the difference between the surface temperature and interior or thermocouple temperature was calculated. If this difference was constant or changed negligibly then the pyrometer measurement was taken to be within its error limit of 1 percent. For example, when the difference between the surface and interior temperature curves in figure 12 was fitted to the least-squares criteria, the maximum deviation from linearity was 3 K. The deviation occurred during a period when the surface was undergoing color changes; thus, probably changes in emissivity. Therefore, the pyrometer temperatures are considered to be accurate to within the basic 1 percent error range of the instrument.

An exact error value cannot be placed on each numeric value of the ignition parameters. However, it is considered that the data accurately represent the temperature of the central region of the specimen where the oxidation events occurred.

Conclusions

The LTS data indicated that milisecond ignition to combustion transitions would not occur at temperatures below the solidus temperature for oxygen pressures up to 6.9 MPa (1000 psia). However, the ignition temperature data

38

have a definite downward trend with increasing oxygen pressure and there were indications of exothermic events occurring at temperatures below the solidus temperature. Therefore, millisecond ignition-to-combustion transitions at temperatures below the solidus temperature and at oxygen pressures greater than 6.9 MPa (1000 psia) cannot be ruled out by using the LTS data. The ITS data, though, do provide this information

The ITS data established that the oxidation rate of the alloy was sufficient for the alloy to autoheat to destruction, under the appropriate experimental conditions, from temperatures below the solidus temperature. (This was independently verified by the DTA data.) These data also indicated that certain oxides, produced during heating, undergo phase changes at various temperatures. As some phase changes occur, apparent increases in oxidation rate of the alloy also occur.

The time required for the development of combustion after ignition decreases as oxygen pressure increases, but does not decrease to the millisecond time frame. Therefore, this alloy did not exhibit an abrupt ignition to combustion transition in the solid state. However, the development of combustion after ignition can be rapid, occurring within several seconds at the higher oxygen pressures. The temperatures at which the ignition parameters occur, decrease with increasing oxygen pressure. This indicates that these parameters are a function of the oxidation rate of the alloy and that the oxidation rate increases more rapidly with increasing oxygen pressure than the cooling rate, which is probably convection controlled.

Future Effort

The program, of which this study is a part, has recently been expanded to include the direct determination of oxidation rates of selected alloys. To

39

achieve this, a thermogravimetric apparatus (TGA), which will use a microgram balance housed in a pressure chamber to directly measure the oxidation rate, is being constructed. The system has been designed to operate to pressures of 34.5 MPa (5000 psia) and to temperatures greater than 1700 K (2600 °F). This equipment will be used to generate oxidation rate data as a function of time, temperature, and oxygen pressure. From these data, the $\dot{Q}$(chem) curve can be determined. Once the $\dot{Q}$(chem) curve is known, computer modeling of system designs and potential abnormal operating conditions can be accomplished and the most appropriate materials chosen.

Acknowledgement

References

[1] Bransford, James W., Billiard, Phillip A., Hurley, James A. and Vazquez Isaura, The Development of Combustion from Quasi-Stable Temperature for the Iron Based Alloy UNS S66286; ASTM SP 986.

[2] Brenner, S.S., Catastrophic Oxidation of Some Molybdenum-Containing Alloys, J. Electrochem. Soc., Vol. 102, No. 1, p. 16 (1954).

[3] Rathenau, G.W. and Meijering, J.L., Rapid Oxidation of Metals and Alloys in the Presence of MoO_3, Metallurgia, Vol. 42, p. 167 (1950).

Appendix: Determination or Probable Emissivity Effects on Spontaneous Ignition

Oxidizing surfaces are notorious for their nonuniform surface emittance. This nonuniformity is in the magnitude of the emittance value at a constant wavelength over time as well as in the variation in emittance value with wavelength and over time.

In our experiments, the variation in emittance with wavelength will affect the accuracy of the surface temperature measurement. However, inaccuracy in this measurement was easily detected by comparing this measurement with that of the interior thermocouple temperature measurement. If the difference between these two measurements was constant or nearly so, then little or no error from emissivity non-linearity was present. For S66286, there were no surface temperature measurement problems, as shown by figure 5 in the text.

The variation of emittance with time at a constant wavelength--the laser wavelength--will affect the heating rate of the specimen. If the variation occurs during a waiting period of an ITS test the effect may appear to be oxidation heating. Therefore, it was necessary to separate the effect of essentially pure oxidation heating on the temperature-time waveform data from the effect of emittance driven heating.

This was accomplished by preoxidizing several specimens in air at temperatures approaching the ignition temperature range. These specimens were then tested using the ITS heating procedure.

A typical result is shown in figure A1. The oxidation heating effect was evidenced by a steadily increasing slope once the effect began. This contrasted with the initial linear or nearly linear increase in the temperature-time waveforms after the beginning of autoheating for non-
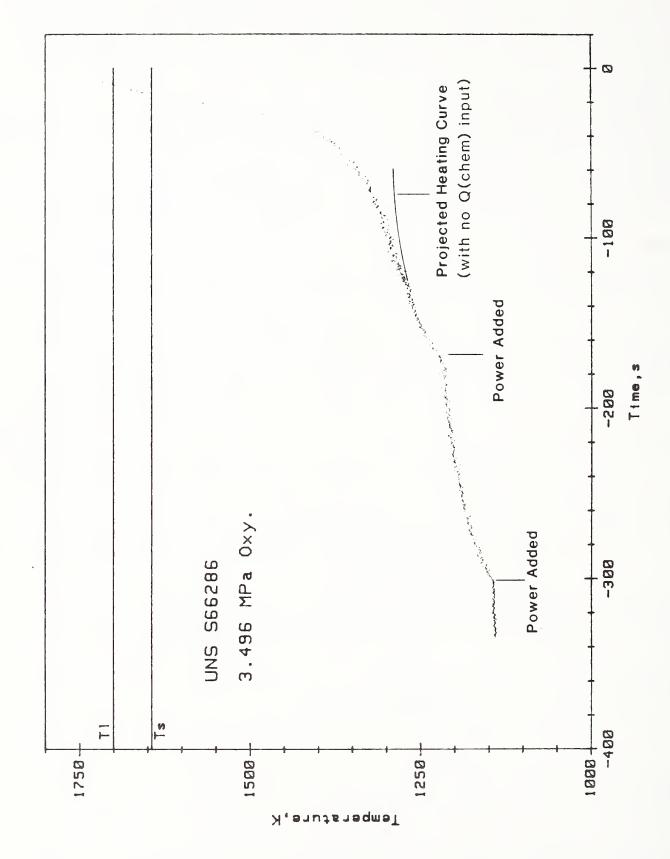
41

Figure A1. Development of ignition using a pre-oxidized specimen.

42

preoxidized test specimens--see figure 5 in the text for an example of a linear waveform segment during autoheating prior to T_{sp}. The conclusion was that the linear or nearly linear waveform segment proceeding the clearly nonlinear segment was due to an increasing absorptivity of the surface to the laser radiation. This increasing absorptivity was probably due almost entirely to increasing emissivity at the laser wavelength in the early stages; but, probably has a surface roughness component in the latter stages.

4. TITLE AND SUBTITLE

Ignition Characteristics of the Iron-Based Alloy UNS S66286 in Pressurized Oxygen

5. AUTHOR(S) James W. Bransford, Phillip A. Billard, James A. Hurley, Kathleen M. McDermott, and Isaura Vazquez

11. ABSTRACT (A 200-word or less factual summary of most significant information. If document includes a significant bibliography or literature survey, mention it here)

The development of ignition and combustion in pressurized oxygen atmospheres was studied for the iron based alloy UNS S66286. Ignition of the alloy was achieved by heating the top surface of a cylindrical specimen with a continuous-wave CO_2 laser. Two heating procedures were used. In the first, laser power was adjusted to maintain an approximately linear increase in surface temperature. In the second, laser power was periodically increased until autoheating (self-heating) was established. It was found that the alloy would autoheat to destruction from temperatures below the solidus temperature. In addition endothermic events occurred as the alloy was heated, many at reproducible temperatures. Many endothermic events occurred prior to abrupt increases in surface temperature and appeared to accelerate the rate of increase in specimen temperature to rates greater than what would be expected from increased temperature alone. It is suggested that the source of these endotherms may increase the oxidation rate of the alloy. Ignition parameters are defined and the temperatures at which these parameters occur are given for the oxygen pressure range of 1.72 to 13.8 MPa (25 to 2000 psia).

12. KEY WORDS (Six to twelve entries; alphabetical order; capitalize only proper names; and separate key words by semicolons)

alloys; combustion; ignition; ignition temperature; iron alloy; metals